# Direct-Current and Alternating-Current Driving Si Quantum Dots-Based Light Emitting Device

Weiwei Mu, Pei Zhang, Jun Xu, Shenghua Sun, Jie Xu, Wei Li, and Kunji Chen

***Abstract*—Light emitting devices based on Si quantum dots/$SiO_2$ multilayers with dot size of 2.5 nm have been prepared. Bright white light emission is achieved under the dc driving conditions and the turn-on voltage of the device is as low as 5 V. The frequency-dependent electroluminescence intensity was observed under ac conditions of square and sinusoidal wave. It was found that the emission wavelength changes with frequency when sinusoidal ac is applied. The degradation of emission intensity is less than 12% after 3 h for ac driving condition, exhibiting the better device stability compared to the dc driving one.**

***Index Terms*—Direct current (dc), electroluminescence (EL), frequency dependent, Si quantum dots (Si QDs).**

## I. Introduction

RECENTLY, Si-based light sources have attracted much attention for their potential applications in realizing on-chip optoelectronic integration. It is well known that the radiative recombination efficiency of bulk Si is very low due to its indirect band structures. In order to circumvent the limit of bulk Si material, various other Si-based materials, such as Si quantum dots (Si QDs), porous silicon, and rare-earth elements doped $SiO_2$ film [1]–[3], have been extensively investigated by researchers. Among these materials, Si QDs have attracted much interest because the radiative recombination possibility of electron–hole (e–h) pairs can be obviously improved due to quantum confinement effect and the emission wavelength can be changed by controlling the dot size [4]. So far, stable and strong photoluminescence (PL) and EL have been observed [5], [6]. For example, Lin *et al.* recently reported the tunable light emission from ITO/$SiO_x$/p-Si/Al LEDs by tailoring the size of Si QDs prepared in plasma-enhanced chemical vapor deposition system (PECVD) [7].

Usually, the electroluminescence (EL) from light emitting devices based on Si QDs is obtained under the dc driving conditions. In order to achieve efficient light emission, high voltage is necessary. However, in that case the charge transport in the oxide takes place mainly via Fowler–Nordheim (FN) tunneling of hot electrons and the e–h pairs are generated by impact ionization of the Si QDs. The FN tunneling of hot carriers will lead to the degradation of the oxide matrix and low device endurance [8]. It has also been reported that under dc driving conditions the charge accumulation occurs at interface states of the contact/active material interface which screens the applied electric field and decreases the effective injection. Peralvarez *et al.* attributed the low emission efficiency of Si-based LEDs to the power dissipation of leakage current through the Si QDs/$SiO_2$ layer instead of injection into the Si QDs [9]. However, by applying ac bias, the mean amount of accumulated charges decreases and the injection becomes more efficient [6]. It means that the applied voltage of ac driven LED can work under relatively low electric field which is helpful for enhancing the emission efficiency, reducing the power consumption as well as improving the device stability [10], [11]. Currently, to develop the Si-based light emitting devices and to study the device performance under dc and ac driving conditions is one of the important issues.

In this paper, we prepared LED containing Si QDs/$SiO_2$ multilayers (MLs). The device performance was systematically investigated under both dc and ac driving conditions. It was demonstrated that low turn-on voltage and strong emission intensity can be achieved. The emission light can be clearly observed. The frequency-dependent EL properties were studied and discussed and good emission stability was obtained for ac driving device.

## II. Experimental Setup

The device was grown on p-type monocrystalline Si wafers with resistivity of 1–3 Ω·cm in a conventional PECVD system with a RF of 13.56 MHz. During the deposition process, the RF power was kept at 50 W and the substrate temperature was fixed at 250 °C. The a-Si:H sublayers were deposited using a pure silane gas with a flow rate of 5 sccm for 15 s. Subsequently, *in situ* plasma oxidation was performed to form ultrathin $SiO_2$ sublayers using oxygen with flow rate of 20 sccm for 90 s. These processes were alternatively changed for nine times and a $SiO_2$ lapping layer was deposited on the top surface of the film. After deposition, the as-grown samples were first dehydrogenated at 450 °C and then annealed at 1000 °C both in $N_2$ ambient for 1 h. In our previous work, we have demonstrated the formation of 2.5 nm Si QDs and 2 nm $SiO_2$ layers [12]–[14]. Then dot-shaped ITO electrodes with diameter of 1.5 mm were deposited on the top of the films and Al electrode was deposited on back of silicon wafer to get EL device. The device was subsequently thermally annealed at 400 °C in $N_2$ for 30 min to set ohmic contacts. The device structure is depicted in the inset of Fig. 1.

Manuscript received January 11, 2013; revised March 11, 2013 and March 19, 2013; accepted March 20, 2013. Date of publication April 29, 2013; date of current version September 18, 2013. This work was supported in part by the 973 Program under Grant 2013CB632101, in part by the NSFC under Grant 61036001 and Grant 11274155, in part by the NSF of Jiangsu Province under Grant BK2010010, and in part by the PAPD.

The authors are with the National Laboratory of Solid State Microstructures and School of Electronic Science and Engineering, Nanjing University, Nanjing 210093, China (e-mail: muww29@gmail.com; zhangpei8157231@163.com; junxu@nju.edu.cn; judeyysun@gmail.com; Jiexu1101@gmail.com; weili@nju.edu.cn; kjchen@nju.edu.cn).

Color versions of one or more of the figures in this paper are available online at http://ieeexplore.ieee.org.

Digital Object Identifier 10.1109/JSTQE.2013.2255587

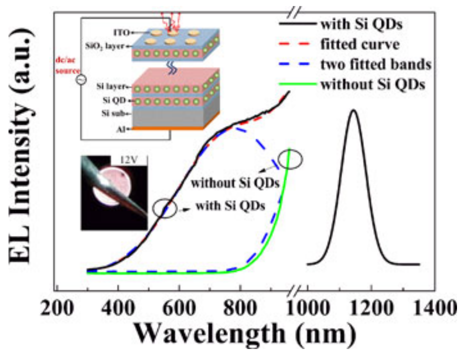


Fig. 1. DC EL spectrum under 12 V in the range of 250–1350 nm. The black lines are detected spectra in visible and infrared range of device with Si QDs. The red dash line is the fitted curve and the blue lines are the two fitted bands. The green line is the EL emission of device without Si QDs. The up inset is the schematic structure of the light emitting device containing $Si/SiO_2$ multilayers; the below one is the EL pattern of our device under applied voltage of 12 V.

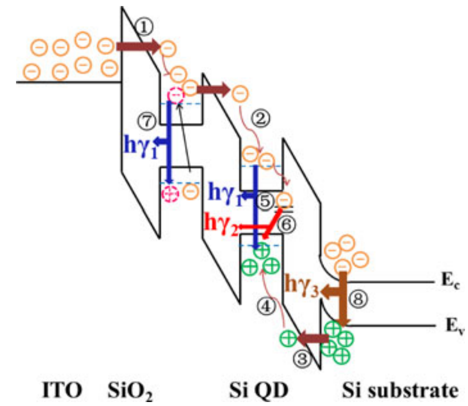


Fig. 2. Schematic diagram of the tunneling and possible light emission routes of our device. ①: FN tunneling of electrons, ②: the relaxation of electrons, ③: FN tunneling of holes, ④: relaxation of holes, ⑤–⑧: the possible recombination routes.

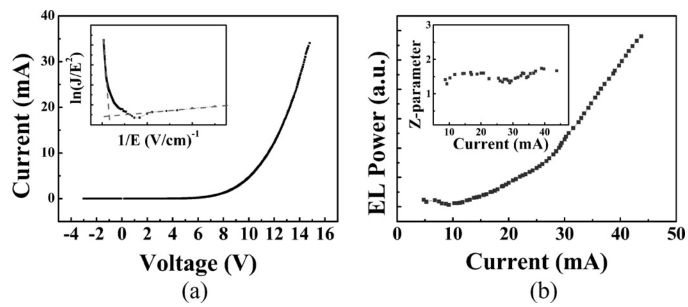


Fig. 3. (a) $I-V$ curve of the device. The inset shows the plot of ln($J/E^2$) as a function of $1/E$; (b) $I-P$ curve and the $Z$ parameter (the inset) of the device.

The EL signals were measured under both dc and ac bias by a HORIBA Jobin Yvon synapse CCD detector in the visible range and a liquid $N_2$ cooled InGaAs detector in the infrared range. The spectra have been calibrated by taking into account the sensitivity of the system.

## III. Results and Discussions

An intense EL can be observed when a forward dc bias was applied to the bottom Al electrode with respect to the top ITO electrode, the EL was uniformly distributed in the whole ITO area. The emitting light became so strong with increasing the applied voltage that it can be seen by naked eyes in the dark room, as shown in the inset of Fig. 1. The LED with low turn-on voltage 1.4–1.7 V was reported by Anopchenko *et al.* previously [6]. The authors ascribed the low voltage to the direct tunneling of carriers other than FN tunneling since it is smaller than the corresponding electrons faced barrier height of 3.2 eV. The turn-on voltage of our device is a little bit higher, which is about 5 V. Fig. 1 also shows the EL spectra of device with Si QDs (black line) and without Si QDs (green line) under the applied dc bias of 12 V in the visible and infrared range. For device with Si QDs, the spectrum is composed of two bands, one is a broadband centered at 750 nm in visible range and the other one at 1150 nm in the infrared range as shown in the right side of Fig. 1. For device without Si QDs (as deposited device), only the band at 1150 nm can be observed and no signal is detected in the visible range.

Fig. 2 depicts the schematic diagram of the possible tunneling and recombination routes in our Si QDs-based device. Under low dc driving conditions, the electrons and holes are injected from ITO electrode and p-Si substrate. The carriers tunneling through the $SiO_2$ barrier layers may recombinate within the Si QDs (process ⑥) or at the Si QDs/$SiO_2$ interfacial states (process ⑤) to emit the visible light. At high voltage, the hot electrons can generate e–h pairs in Si QDs by impact ionization and the recombination of e–h pairs in Si QDs and/or Si QDs/$SiO_2$ interfacial states can also emit the visible light (process ⑦). In addition, we found that the EL peak in visible light region can be slightly red-shifted with increasing Si QD size to 4 nm (the results are not shown here), which can be ascribed to the quantum confinement effect as proposed by Park *et al.* [4]. Qin *et al.* attributed this visible light emission to the nc-Si/$SiO_2$ interfacial states based on the PL results [15]. As for the EL band in the infrared region, it can be attributed to the band edge emission from p-Si substrate (process ⑧). It has been reported that efficient EL can be observed from metal/ultrathin $SiO_2$/p-Si tunnel diodes [16], [17]. The negative gate bias can attract the holes at the Si/$SiO_2$ interface to form the accumulation region. The holes are localized along the growth direction and their momentum spread in $k$-space. Consequently, light emission occurs at $SiO_2$/p-Si substrate interface when the electrons reach the p-Si substrate and the quantum efficiency of band edge emission is higher than that of bulk Si [16].

According to the current–voltage $(I-V)$ curve shown in Fig. 3(a), we found that the carrier transport in our device is mainly dominated by the direct tunneling at the low voltage regime [$\sim$7.2 V, corresponding to the electric field of 1.6 MV/cm by concerning the total film thickness of 45 nm, as shown in the inset of Fig. 3(a)]. The EL emission comes from the recombination of bipolar injected electrons and holes as discussed previously [8]. We also measured the EL under the reverse bias (the gate is positively biased), no EL signal can be detected even at high applied voltage, which indicates that the impact ionization does not contribute significantly to the EL emission [6]. However, at high forward voltage, the carrier transport is dominated by the FN tunneling mechanism and the electrons can gain sufficient energy to generate e–h pairs in Si QDs by impact ionization. Then the recombination of hot electrons generated e–h pairs emits the visible light. Marconi *et al.* have studied the EL of Si QDs/$SiO_2$ multilayers, they found that when the electric field is less than 2 MV/cm (also they used the total film thickness to estimate the electric field), the charge injection is attributed to the bipolar injection into silicon nanocrystals via direct tunneling [8]. While in the case of high voltages, the FN tunneling dominates in the charge injection process. In this regime, the charge transports in the oxide mainly via hot electrons and the e–h pairs are generated by impact ionization in the nc-Si, which will lower the power efficiency.

Fig. 3(b) shows the EL power as a function of the injected current. Only the EL intensity of the band centered at 750 nm is integrated to estimate the output EL power. Theoretically, the dominant process of recombination in LED can be described by $Z$ parameter according to the *P–I* curve [18]–[20]. In the steady state, the injected current balances the net recombination when stimulated emission is neglected. This balance can be expressed as

$$I_{\text{total}} = eV_a(\text{AN} + \text{BN}^2 + \text{CN}^3) \tag{1}$$

where $I_{\text{total}}$ is the total current, $e$ is the electronic charge, $V_a$ is the active volume, and A, B, C are coefficients associated with defect, radiative, and Auger related recombination, respectively, $N$ is the carrier concentration.

Given the different current dominating in total current, equation (1) can be written as

$$I_{\text{total}} \propto N^Z \tag{2}$$

where $Z$ may range from 1 to 3 for different recombination mechanisms. For defect, radiative, and Auger dominated recombinations the $Z$ parameter is 1, 2, and 3, respectively.

Moreover, the rate equation for e–h recombination with an external supplied current density of $J$ is described as

$$\frac{d[n(J)]}{d[t]} = \frac{J}{ed} - \frac{n}{\tau} \tag{3}$$

where $d$ is the recombination thickness and $\tau$ is the carrier lifetime. At steady state, $d[n]/d[t] = 0$, we obtain

$$n = \frac{\tau J}{ed} \tag{4}$$

then the internal optical power can be written as

$$P = \eta_{\text{internal}} \frac{hcI}{e\lambda} = \text{BN}^2 V_a \frac{hc}{\lambda}. \tag{5}$$

Consequently, using (2) and (5), the relationship between $P$ and $I_{\text{total}}$ is

$$P^{Z/2} \propto I_{\text{total}}. \tag{6}$$

Then $Z$ parameter can be obtained from the derivation of the $\ln(I)$ verse $\ln(P^{1/2})$ plot [20].

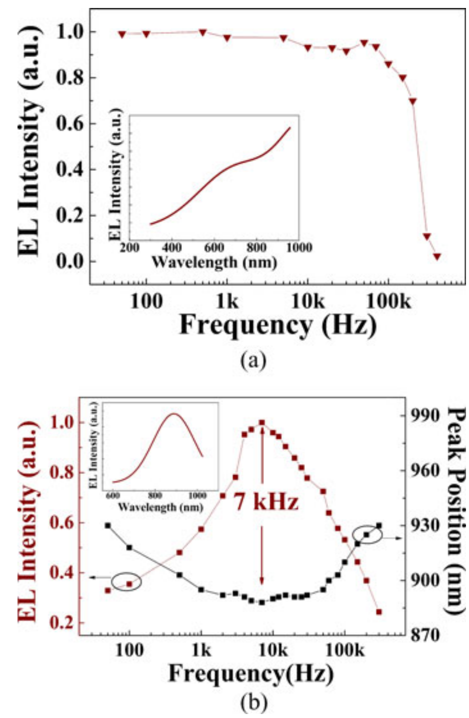


Fig. 4. (a) Normalized EL intensity under ac (square wave) driving conditions as a function of frequency. The inset is the spectrum under 14 V at 7 kHz. (b) Normalized EL intensity under ac (sin wave) driving conditions as a function of frequency (red line); the peak center position as a function of frequency (blue line). The inset shows the EL spectrum under 14 V at 7 kHz.

In our case, the $Z$ parameter is about 1.5 as shown in the inset of Fig. 3(b), which indicates that defect and radiative recombination are the two dominant recombination processes. It means that both the recombination of e–h pairs within Si QDs and via Si QDs/$SiO_2$ interfacial defect states contribute to the broad EL spectra as shown in Fig. 1. The $Z$ parameter has not been above 2 even at large current, suggesting that Auger recombination has not yet dominated in our device.

It is interesting to study the device performance under ac driving conditions. The inset of Fig. 4(a) shows the EL spectrum of the device measured under square ac voltages with voltage of 14 V at 7 kHz. It is very similar with the dc driving one and is composed of two bands, too. This is comprehensible since the applied voltage is quite similar with dc. The frequency-dependent intensity is summarized in Fig. 4 with $V_{\text{rms}}$ kept at 14 V and frequency increased from 50 Hz to 200 kHz. The intensity barely changes when frequency is below 50 kHz and above that the carrier transportation cannot keep up with the change of the voltage, resulting in the dramatic decrease in EL intensity.

When sinusoidal wave ac is applied, as shown Fig. 4(b), we can see that the EL intensity is also frequency dependent. The EL intensity increases at first with increasing the frequency from 50 Hz to 7 kHz and then reduced with further increasing the frequency from 7 to 200 kHz. The similar result was also reported in device based on $Si^+$ ion implanted MOS-like (poly-Si/$SiO_2$/Si) structure [21]. The reason for the intensity increasing at first is that the carriers have more chances to inject and recombine in the same time period as frequency increase, and the premise here is that the movement of carriers can keep up with alternation of ac voltages. When the frequency gets as high as 7 kHz, which corresponds to the time scale of the carrier tunneling time into neutral Si QDs, the EL intensity reaches its maximum [22]–[24].

As the frequency is increased from 7 to 50 kHz, carriers tunneling will lag the changing of the voltages. Thus, electrons and holes will have a lower possibility to encounter and that will lead to the decrease in EL intensity, as mentioned in square wave driving condition. Beyond 50 kHz, the first injected carriers (e/h) will be electrically pumped out before they can recombine with the latter ones (h/e) since the nc-Si radiative recombination lifetime is about 25 $\mu$s, as reported by Walters *et al.*, and the sharp decrease in EL intensity is inevitable. The authors also found that the EL intensity showed a peak at 10 kHz and they believe that it corresponds to the performance-limiting charge injection timescale for the first carriers into the neutral nanocrystals of $\sim$50 $\mu$s. At the frequency above $\sim$30 kHz, the pulse duration becomes shorter than the radiative lifetime of silicon nanocrystals and some of the excitons do not recombine, which leads to the decrease in EL intensity. The small discrepency with our device may be due to the different device structure and the surrounding environment of Si QDs.

As the frequency is increased from 7 to 50 kHz, carriers tunneling will lag the changing of the voltages. Thus, electrons and holes will have a lower possibility to encounter and that will lead to the decrease in EL intensity, as mentioned in square wave driving condition. Beyond 50 kHz, the first injected carriers (e/h) will be electrically pumped out before they can recombine with the latter ones (h/e) since the nc-Si radiative recombination lifetime is about 25 $\mu$s, as reported by Walters *et al.*, and the sharp decrease in EL intensity is inevitable. The authors also found that the EL intensity showed a peak at 10 kHz and they believe that it corresponds to the performance-limiting charge injection timescale for the first carriers into the neutral nanocrystals of $\sim$50 $\mu$s. At the frequency above $\sim$30 kHz, the pulse duration becomes shorter than the radiative lifetime of silicon nanocrystals and some of the excitons do not recombine, which leads to the decrease in EL intensity. The small discrepency with our device may be due to the different device structure and the surrounding environment of Si QDs.

At the same time, the slight frequency-dependent peak position was observed with position change of 40 nm, i.e., 0.06 eV in energy. As summarized in Fig. 4(b), the EL peak is centered at 930 nm at the measurement frequency of 50 Hz, and it gradually shifts to 890 nm with increasing the frequency to 7 kHz. As further increasing the frequency to 200 kHz, the EL peak shows an opposite change that the peak returns gradually to 930 nm. Compared to dc driving conditions, the EL peaks are red-shifted under ac (sin) conditions. This may be due to the fact that carriers can be accelerated toward one direction and tunnel into Si QDs, then these hot carriers recombinate in Si QDs under dc conditions. While in ac (sin) conditions, the carriers cannot tunnel into Si QDs and instead they can only recombinate via the lower defect states in nc-Si/$SiO_2$ interfaces. The bulk Si related peak at 1150 nm observed under dc bias

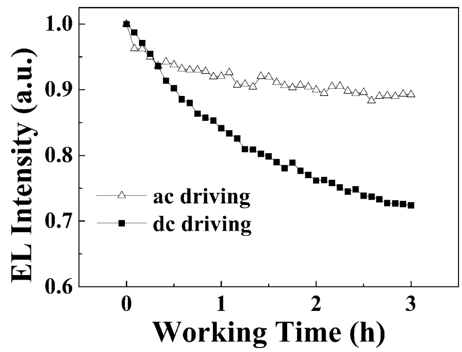


Fig. 5. Stability of our device under dc and ac driving conditions in the elapsed working time of 3 h with a constant applied voltage of 20 V.

is suppressed does not appear here when ac bias is applied. This can be attributed to the alternative injection of carriers that holes do not have enough time to accumulate at the interface and emit the band edge light before being repelled. The integrated EL intensity under sinusoidal ac bias is 3.4 times as strong as that under dc bias at the same voltage, which means that EL efficiency in visible range is obviously enhanced. The mechanism of frequency-dependent EL peak shift in our devices is still unclear at the present stage. Yeh *et al.* reported the similar frequency-dependent peak position shifting phenomenon in intrinsic amorphous silicon nitride (a-Si:N:H) film [25]. They found that EL peak wavelength shifted toward longer one with increasing frequency from 60 Hz to 50 kHz, and then it kept at a fixed wavelength even though the frequency was further increased. They believe that it is due to the changing of the place where the carriers recombine. In our case, as we mentioned earlier, both the recombination of e–h pairs within Si QDs and through the interfacial states contributes to the final EL spectra. The shift of EL peak may be ascribed to the competition between these two recombination processes. But it needs further investigation on $Z$ parameter. The detailed discussion depends on systematical measurements of *P–I* relationship under various frequencies, which will be addressed later.

Fig. 5 shows the normalized EL intensity of the device operated under dc and 1 kHz sinusoidal ac conditions, both at constant voltage of 20 V. The currents barely changed in the measurement process. We can see that the device exhibits good stability under both conditions in the whole elapsed 3 h. The EL intensities keep at 70% and 88% of their original ones under dc and ac conditions after 3 h and almost saturate. Matsuda *et al.* have reported the time dependence of ac EL intensity at various frequencies $n^+$-poly silicon/Si implanted $SiO_2$/p-Si MOS capacitors. They found that the device showed poor stability at low frequencies and it performed the best at 100 kHz. However, the EL intensity had only about 60% of its initial intensity after 90 min [11]. The reason for the excellent stability of our device may due to the well-preserved multilayered structure even under high voltage. For the ac driving condition it shows better stability. In ac driving conditions, the flowing current is lower than that in dc driving conditions under the some applied voltage and the device has been on less operation time which results in the less thermal degradation of device. Moreover, in ac bias at the same voltage it has been on less operation time which results in the less thermal degradation of device. Also, the trapped charges can be extracted in each period resulting in less defect creation which is also helpful for improving the device endurance.

## IV. Conclusion

We fabricated the light emitting devices based on Si QDs/$SiO_2$ multilayers with dot size of 2.5 nm. The stable and strong EL can be observed from our devices under the dc and ac driving conditions. The turn-on voltage of the devices is as low as 5 V and the luminescence wavelength is centered at 750 nm due to the recombination of injected electrons and holes in Si QDs or at the Si QDs/$SiO_2$ interfacial states. Under the ac driving conditions, the different frequency-dependent EL peak and intensity was found for square and sinusoidal ac conditions, which can be attributed to the modulation of tunneling time of carriers, especially electrons. The good light emission stability has been achieved in our devices under the ac driving conditions. That indicates that the Si-based light emitting devices can be potentially applied for future Si-based optoelectronic integration.

## References

[1] T. W. Kim, C. H. Cho, B. H. Kim, and S. J. Park, "Quantum confinement effect in crystalline silicon quantum dots in silicon nitride grown using $SiH_4$ and $NH_3$," *Appl. Phys. Lett.*, vol. 88, p. 123102, 2006.

[2] M. Meneghini, M. Scamperle, and M. Pavesi, "Electron and hole-related luminescence processes in gate injection transistors," *Appl. Phys. Lett.*, vol. 97, p. 033506, 2010.

[3] G.-R. Lin, C.-J. Lin, and C.-T. Lin, "Low-plasma and high-temperature PECVD grown silicon-rich $SiO_x$ film with enhanced carrier tunneling and light emission," *Nanotechnology*, vol. 18, p. 395202, 2007.

[4] N.-M. Park, T.-S. Kim, and S.-J. Park, "Band gap engineering of amorphous silicon quantum dots for light-emitting diodes," *Appl. Phys. Lett.*, vol. 78, pp. 2575-1–2575-3, 2001.

[5] G. Franzò, M. Miritello, S. Boninelli, R. Lo Savio *et al.*, "Microstructural evolution of $SiO_x$ films and its effect on the luminescence of Si nanoclusters," *J. Appl. Phys.*, vol. 104, p. 094306, 2008.

[6] A. Anopchenko, A. Marconi, E. Moser, L. Pavesi *et al.*, "Low-voltage onset of electroluminescence in nanocrystalline-Si/$SiO_2$ multilayers," *J. Appl. Phys.*, vol. 106, pp. 033104-1–033104-8, 2009.

[7] B.-H. Lai, C.-H. Cheng, and G.-R. Lin, "Multicolor ITO/$SiO_x$/p-Si/Al light emitting diodes with improved emission efficiency by small Si quantum dots," *IEEE J. Quantum Electron.*, vol. 47, no. 5, pp. 698–704, May 2011.

[8] A. Marconi, A. Anopchenko, M. Wang, G. Pucker, P. Bellutti *et al.*, "High power efficiency in Si-nc/$SiO_2$ multilayer light emitting devices by bipolar direct tunneling," *Appl. Phys. Lett.*, vol. 94, p. 221110, 2009.

[9] M. Perálvarez, C. García, M. López, and B. Garrido, "Field effect luminescence from Si nanocrystals obtained by plasma-enhanced chemical vapor deposition," *Appl. Phys. Lett.*, vol. 89, p. 051112, 2006.

[10] T. Matsuda, H. Takata, M. Kawabe, and T. Ohzone, "Electroluminescence of MOS capacitors with Si-implanted $SiO_2$," *Solid-State Electronics*, vol. 41, pp. 887–893, 1997.

[11] T. Matsuda, H. Takata, M. Kawabe, and T. Ohzone, "Visible electroluminescence from MOS capacitors with Si-implanted $SiO_2$ under dynamic operation," in *Proc. Electron Devices Meeting*, pp. 8.2.1–8.2.4, 2001.

[12] H. C. Sun, J. Xu, Y. Liu, W. W. Mu, W. Xu, W. Li, and K. J. Chen, "Subband light emission from phosphorous-doped amorphous Si/$SiO_2$ multilayers at room temperature," *Chin. Phys. Lett.*, vol. 28, p. 067802, 2011.

[13] D. Y. Chen, D. Y. Wei, J. Xu, and P. G. Han, "Enhancement of electroluminescence in p–i–n structures with nano-crystalline Si/$SiO_2$ multilayers," *Semicond. Sci. Technol.*, vol. 23, p. 015013, 2008.

[14] J. Zhou, G. R. Chen, Y. Liu, and J. Xu, "Electroluminescent devices based on amorphous SiN/Si quantum dots/amorphous SiN sandwiched structures," *Opt. Exp.*, vol. 17, p. 158, 2009.

[15] G. G. Qin, S. Y. Ma, Z. C. Ma, W. H. Zong, and L. P. You, "Electroluminescence from amorphous Si/$SiO_2$ superlattices," *Solid State Commun.*, vol. 106, pp. 329–333, 1998.

[16] M. Sopinskyy and V. Khomchenko, "Electroluminescence in $SiO_x$ films and $SiO_x$-film-based systems," *Current Opinion Solid State Mater. Sci.*, vol. 7, pp. 97–109, 2003.

[17] J. Xu, K. Makihara, H. Deki, and S. Miyzazki, "Electroluminescence from Si quantum dots/$SiO_2$ multilayers with ultrathin oxide layers due to bipolar injection," *Solid State Commun.*, vol. 149, pp. 739–742, 2009.

[18] R. Fehse, S. Tomic, A. R. Adams, S. J. Sweeney, E. P. O'Reilly, A. Andreev, and H. Riechert, "A quantitative study of radiative, auger, and defect related recombination processes in 1.3-$\mu$m GaInNAs-based quantum-well lasers," *IEEE J. Select. Topics Quantum Electron.*, vol. 8, no. 4, pp. 801–810, Jul./Aug. 2002.

[19] L. L. Goddard, S. R. Bank, M. A. Wistey, H. B. Yuen, H. P. Bae, and J. S. Harris, Jr., "Reduced monomolecular recombination in GalnNAsSb/GaAs lasers at 1.5$\mu$m," in *Proc. IEEE The 17th Annual Meeting Lasers and Electro-Opt. Soc.*, 2004, pp. 144–145.

[20] C.-H. Cheng, C.-L. Wu, C.-C Chen, L.-H. Tsai, Y.-H. Lin, and G.-R. Lin, "Si-Rich $Si_xC_{1-x}$ light-emitting diodes with buried Si quantum dots," *IEEE Photonics J.*, vol. 4, no. 5, pp. 1761–1775, 2012.

[21] V. Beyer, B. Schmidt, K.-H. Heinig, and K.-H. Stegemann, "Light emitting field effect transistor with two self-aligned Si nanocrystal layers," *Appl. Phys. Lett.*, vol. 95, p. 193501, 2009.

[22] R. J. Walters, G. I. Bourianoff, and H. A. Atwater, "Field-effect electroluminescence in silicon nanocrystals," *Nature Mater.*, vol. 4, pp. 143–146, 2005.

[23] R. J. Walters, J. Carreras, T. Feng, L. D. Bell, and H. A. Atwater, "Silicon nanocrystal field-effect light-emitting devices," *IEEE J. Sel. Topics Quantum Electron.*, vol. 12, no. 6, pp. 1647–1656, Nov./Dec. 2006.

[24] J. Carreras, J. Arbiol, B. Garrido, C. Bonafos, and J. Montserrat, "Direct modulation of electroluminescence from silicon nanocrystals beyond radiative recombination rates," *Appl. Phys. Lett.*, vol. 92, p. 091103, 2008.

[25] R.-H. Yeh, T.-R. Yu, T.-C. Chung, S.-Y. Lo, and J.-W. Hong, "Optoelectronic characteristics of direct-current and alternating-current white thin-film light-emitting diodes based on hydrogenated amorphous silicon nitride film," *IEEE Trans. Electron Devices*, vol. 55, no. 4, pp. 978–985, Apr. 2008.

**Weiwei Mu** was born in Yancheng, Jiangsu, China, in 1988. He received the B.S. degree in physics from Nanjing University, Nanjing, China, in 2010, where he is currently working toward the M.S. degree in the field of silicon-based optoelectronic device.

**Pei Zhang** received the B.S. degree from Huanghuai University, Zhumadian, China, in 2008 and the M.S. degree in physical electronics from Huaqiao University, Quanzhou, Chian, in 2011. He is currently working toward the Ph.D. degree in microelectronics at Nanjing University, Nanjing, China.

His current research interests include optical nonlinear properties of silicon nanocrystals.

**Jun Xu** received the B.S. degree in physics and the Ph.D. degree in microelectronics both from Nanjing University, Nanjing, China, in 1989 and 1995, respectively.

In 1996, he was a member of the National Laboratory of Solid State Microstructures, Nanjing University. Since 2004, he has been a Professor in the Department of Phyics and School of Electronic Science and Engineering. He worked as a Visiting Researcher in the Department of Electronic Engineering, Hongkong Chinese University, in 2000 and the Graduate School of Advanced Science of Matter, Hiroshima University, Japan, in 2005. His research interests include silicon-based amorphous materials, semiconductor nanostructures, and optoelectronic devices.

**Shenghua Sun** received the B.S. degree in microelectronics from Nanjing University, Nanjing, China, in 2006, where he is currently working toward the M.S. degree in microelectronics.

His research interests include the fabrication of Si nanopatterned structures and the application in Si quantum dots solar cells.

**Jie Xu** received the B.S. degree in electronic science and engineering from Nanjing University, Nanjing, China, in 2011, where he is currently working toward the Ph.D. degree in electronic science and engineering.

His current research interests include silicon-based optoelectronic devices.

**Wei Li** received the B.S. degree in electronic and automatic control from Nanjing University, Nanjing, China, in 2002.

He was with the School of Electronic Science and Engineering, Nanjing University, in 2010. His current research interests include material growth and characterization of silicon-based optoelectronic and electronic device.

**Kunji Chen** received the Graduate degree from Nanjing University, Nanjing, China, in 1963.

From 1981–1983, he was a Visiting Scholar studying at the University of Chicago, Chicago, IL, USA. Since then he had eight times to go to the Universities and Institutes of United State and Japan for cooperation research work. He is currently a Professor at Nanjing University. He has published more than 350 articles and one book and owns 12 invention patents. His research interests include nanosemiconductor materials, quantum nanoelectronics, and nanooptoelectronics.

Prof. Chen has received many awards including the National Nature Science Award in 2003 and the Advanced Achievements Award in Science and Technology of Jiangsu Province (1988, 1995, and 2002). In 1996, he was elected as a member of the International Advisory Committee of International Conference on Amorphous and Nanocrystalline Semiconductors (ICANS).